

Localization Phenomena in Large-Scale Networked Systems: Implications for Fragility

Poorva Shukla and Bassam Bamieh

Abstract—We study phenomena where some eigenvectors of a graph Laplacian are largely confined in small subsets of the graph. These localization phenomena are similar to those generally termed Anderson Localization in the Physics literature, and are related to the complexity of the structure of large graphs in still unexplored ways. Using spectral perturbation theory and pseudo-spectrum analysis, we explain how the presence of localized eigenvectors gives rise to fragilities (low robustness margins) to unmodeled node or link dynamics. Our analysis is demonstrated by examples of networks with relatively low complexity, but with features that appear to induce eigenvector localization. The implications of this newly-discovered fragility phenomenon are briefly discussed.

I. INTRODUCTION AND PROBLEM SETTING

The phenomenon of Anderson localization is well known in condensed-matter physics. The original work [1] from the late 50's received the Physics Nobel prize in 1977, and it remains an active and important area of research to this day. In physics, it refers to the abrupt change of the nature of eigenfunctions in the presence of disorder (randomness) in the governing potentials in quantum-mechanical or classical models. For certain models, arbitrarily small amounts of disorder can cause eigenfunctions to change from being “delocalized” (having their mass distributed globally in space) to having exponential decay, i.e. becoming “localized” in space. This can translate to abrupt changes in material properties. In this sense, localization phenomena can be broadly understood as those of “fragilities” of certain mathematical models of reality.

It has recently been recognized that localization phenomena are much more ubiquitous than previously thought, and can occur not only due to randomness in media, but also due to complex geometry of boundaries in non-random problems [2]. It has also been observed in acoustic systems where localization occurs due to fractal boundaries [3], or inhomogeneity in the medium [4]; and bio-molecular vibrations [5] where localization is caused due to the spatial complexity of 3D protein structures. Therefore it may be suspected that localization phenomena can occur in other mathematical models of the dynamics of large-scale systems and networks such as in neuroscience, power grids, multi-agent systems, vehicular and robotic networks among others.

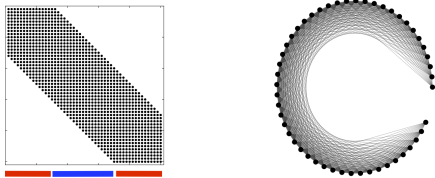
In this paper we introduce the concept of eigenvector localization in the context of graph Laplacians. Characterizing which graphs poses this property requires a much lengthier analysis and will be reported elsewhere [6]. In this paper we instead address the following system-theoretic question:

Authors are with the Department of Mechanical Engineering, University of California at Santa Barbara. {poorvashukla,bamieh}@ucsb.edu

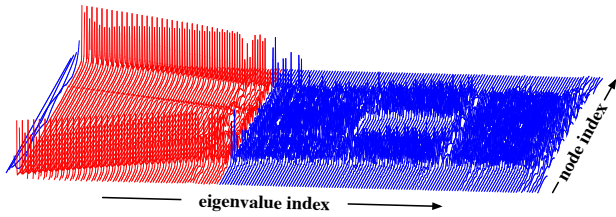
Given a graph where some of its Laplacian's eigenvectors have the localization property, what effects does this property have on robustness/fragility of networked dynamical systems defined over this graph. In particular, we examine 2nd-order “consensus-type” systems such as the swing equations of power networks, vehicular formations, or networked 2nd-order linear oscillators in general. We consider various types of dynamical node and edge perturbations and examine their effects on overall system stability using large-scale examples, and a spectral perturbation analysis which provides some theoretical guidance.

We now give an informal description of the localization phenomenon by way of the example in Figure 1. Formal definitions will be given in later sections. Figure 1a shows a network with $N = 50$ nodes, and Figure 1b shows an overview of the Laplacian's eigenvectors for a network with the same structure but with $N = 200$. Roughly about 80 of those eigenvectors (depicted in red) appear to be “localized”, i.e. most of their mass is concentrated over a very small number of nodes, while the remaining eigenvectors (depicted in blue) are spread out over a large subdomain. This contrast in structure of localized versus delocalized eigenvectors is shown more clearly for two specific eigenvectors in Figure 1c. The main feature is that localized eigenvectors decay rapidly (with respect to node index) away from their peak. Note that in Figure 1b the eigenvectors indices are ordered in increasing magnitude of eigenvalues, and the localized ones appear to be towards the bottom of the spectrum. Other examples, not reported here due to lack of space, exhibit localization in other portions of the spectrum depending on the graph structure. Furthermore, the localized eigenvectors appear to have most of their masses in particular regions of the graph (depicted with the red bars in Figure 1a), with the complementary subregion having delocalized eigenvectors whose mass is widely spread in that region (depicted with the blue bar). We call such regions of the graph the “localized” and “delocalized” regions respectively.

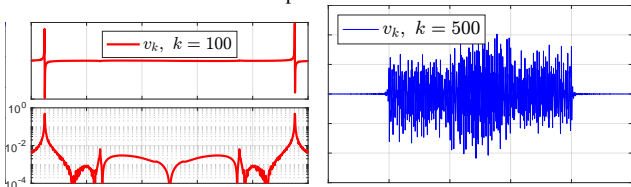
The question we investigate in this paper concerns robustness of dynamical systems defined on graphs whose Laplacians possess localized eigenvectors like those of the example of Figure 1. *Is the system more fragile when there is uncertainty in node/link dynamics within a localized region compared to those in a delocalized region?* We show with examples that the answer is in the affirmative, and provide a perturbation analysis to support this conclusion for any graph with localized Laplacian eigenvectors. The perturbation analysis also implies that this fragility contrast (between localized and delocalized perturbations) can become arbitrarily large



(a) A network (*right*) with equal edge weights corresponding to a banded Laplacian (shown on *left*). $N = 50$ and band size = 30 is chosen for ease of visualization.



(b) A plot of all the eigenvectors of the same network structure as (a) with $N = 200$ and band size ≈ 80 . The red lines show localized eigenvectors, while the blue lines are delocalized eigenvectors. The eigenvectors are plotted in increasing magnitude of eigenvalues, and the localized ones are towards the bottom end of the spectrum.



(c) Same example with $N = 1000$ and band size 200. (*Left*) A localized eigenvector plotted with absolute and semi-log scales. (*Right*) A typical delocalized eigenvector that has substantial magnitude over a large subdomain. In all the three plots the x -axis is the node index.

Fig. 1: An example illustrating Laplacian eigenvector localization. A subset of the eigenvectors are localized, while others are not.

in the limit of large network size. Given the ubiquity of localization phenomena as mentioned in the introductory paragraphs, we argue that these robustness/fragility issues deserve further careful examination in dynamical networks problems.

This paper is organized as follows. In section II, we recall some preliminary facts about graph Laplacians and small-gain robustness analysis in the context of LTI systems and H^∞ norms. Section III considers the network of Figure 1 in the context of a 2nd-order oscillator model, and illustrates the relative fragility for dynamic perturbations in the localized versus the delocalized regions of the graph. Section IV gives a formal definition for eigenvector localization, then develops spectral perturbation analyses to demonstrate that the conclusions from this example are likely to be generic whenever network Laplacians exhibit localization of subsets of their eigenvectors. To the best of our knowledge, this observation has not been made in the cooperative/networked/distributed control literature. The final Section V reprises some conclusions and the many remaining open questions.

II. PRELIMINARIES

We denote an *undirected* graph by (\mathbb{G}, \mathbb{E}) where \mathbb{G} is the set of nodes and \mathbb{E} is the set of edges, i.e. for nodes $i, j \in \mathbb{G}$, $(i, j) \in \mathbb{E}$ if there is an edge connecting nodes i and j . The

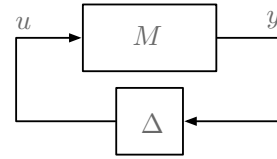


Fig. 2: The setting of the robust stability small-gain theorem.

Laplacian matrix of an undirected graph is defined as $\mathcal{L} := D - A$, where A is the adjacency matrix and D is the diagonal matrix of node degrees [7]. In this case the eigenvalues of \mathcal{L} are all non-negative, and all but the smallest are positive if the graph is connected, which we assume throughout.

Let H^∞ be the Banach space of Single-Input-Single-Output (SISO) continuous-time, real-coefficient, L^2 -stable transfer functions [8]. For any such system M we use the following notation for its H^∞ norm

$$\|M\|_\infty := \sup_{s \in \text{RHP}} |M(s)|,$$

where $|M(s)|$ is the modulus of the complex number $M(s)$, and $\text{RHP} := \{s \in \mathbb{C}; \text{Re}(s) \geq 0\}$.

A. LTI Small Gain Theorem

The Linear Time Invariant (LTI) small-gain theorem concerns the robust stability of the feedback system of Figure 2 for two equivalent classes of perturbations Δ .

Theorem 2.1: The feedback system of Figure 2 is stable for all $\Delta \in H^\infty$ with $\|\Delta\|_\infty \leq \varepsilon$ iff

$$\|M\|_\infty < 1/\varepsilon. \quad (1)$$

Equivalently, it is stable $\forall \Delta \in \mathbb{C}$ with $|\Delta| \leq \varepsilon$ iff (1) holds.

Note that $\Delta \in H^\infty$ are LTI systems with real coefficients, while $\Delta \in \mathbb{C}$ represents static, but complex feedback gains. Testing robust stability with complex gains $\Delta \in \mathbb{C}$ is mathematically easier, but physical interpretations are of course more reasonable when considering perturbations $\Delta \in H^\infty$.

When the condition $\|M\|_\infty < 1/\varepsilon$ is violated, it is useful to exhibit specific dynamic systems $\Delta \in H^\infty$ with $\|\Delta\|_\infty \leq 1/\varepsilon$ that destabilize the feedback systems. If M achieves its H^∞ norm at $s = 0$ or $s = \infty$, then a simple (real) static proportional gain $\Delta = 1/\|M\|_\infty \leq \varepsilon$ will destabilize the system. Otherwise, there are standard constructions of destabilizing dynamic perturbations. For example, let $\bar{\omega}$ be the frequency at which M achieves its H^∞ norm, and assume for simplicity that M is Single Input Single Output (SISO), i.e.

$$M(j\bar{\omega}) = |M(j\bar{\omega})| e^{j\angle M(j\bar{\omega})}, \quad |M(j\bar{\omega})| \geq 1/\varepsilon,$$

where $\angle M(j\bar{\omega})$ is the phase of M at $j\bar{\omega}$. Then a delay perturbation of the form

$$\Delta(s) = \frac{1}{\|M\|_\infty} e^{-Ts}, \quad T = \angle M(j\bar{\omega})/\bar{\omega}$$

will cause $1/(1 - M(s)\Delta(s))$ to have a pole at $s = j\bar{\omega}$, thus destabilizing the feedback system. Note that $\|\Delta\|_\infty = 1/\|M\|_\infty \leq \varepsilon$ as required. Alternatively, a first-order, non-minimum phase Δ with real coefficients can be constructed [9, Thm. 8.1] to destabilize the system. Note that a

1st-order non-minimum phase system acts like a “dynamical delay”, i.e. it is delay-type perturbations in feedback that typically destabilize LTI systems.

The quantity $1/\|M\|_\infty$ above is sometimes referred to as the “robust stability margin” of the feedback system of Figure 2.

B. The Structured Pseudo-spectrum

When M is given in terms of a state-space realization

$$M : \begin{cases} \dot{x} &= Ax + Bu, \\ y &= Cx, \end{cases} \quad (2)$$

the stability margin can be given in terms of properties of the matrix triple (A, B, C) . Consider the following definition.

Definition 2.2: Given matrices (A, B, C) of compatible dimensions, the *structured ε -pseudospectrum* of this triple is

$$\sigma_\varepsilon(A, B, C) := \{ \sigma(A + B\Delta C); \Delta \in \mathbb{C}^{p \times q}, \|\Delta\| \leq \varepsilon \},$$

where $\sigma(H)$ stands for the spectrum of a matrix H and $\|\cdot\|$ is the standard 2-norm of a matrix.

This is a generalization of the ε -pseudospectrum [10]. When $\varepsilon = 0$, it is just the spectrum of A , and for $\varepsilon > 0$ it can be thought of as a “thickened spectrum” of A as determined by the interaction between the triple of matrices (A, B, C) . It is easy to show [11] that the structured ε -pseudospectrum is the *super-level-set* of a transfer function

$$\sigma_\varepsilon(A, B, C) = \{ s \in \mathbb{C}; \|C(sI - A)^{-1}B\| \geq 1/\varepsilon \}. \quad (3)$$

This is the transfer function of the system M in (2), and therefore we can now relate the structured ε -pseudospectrum, and the robust stability conditions of the small-gain theorem.

Theorem 2.3: Consider the feedback system of Figure 2 where M has the state-space realization (2). The feedback system is robustly stable for all $\Delta \in \mathbb{H}^\infty$, $\|\Delta\|_\infty \leq \varepsilon$ iff

$$\sup \left\{ \operatorname{Re} \left(\sigma_\varepsilon(A, B, C) \right) \right\} < 0,$$

i.e. iff the structured ε -pseudospectrum does not intersect the (closed) RHP.

This theorem follows (in the SISO case) from simply observing that the robust stability condition (1)

$$\sup_{s \in \text{RHP}} |C(sI - A)^{-1}B| \leq 1/\varepsilon$$

holds iff the set (3) does not intersect the RHP.

Theorem 2.3 provides for a graphical depiction of robustness (or fragility) margins by plotting the structured ε -pseudospectrum of a system in the complex plane for various types of perturbations, and observing its distance from the RHP.

III. PERTURBATIONS IN LOCALIZED VS. DELOCALIZED REGIONS: NETWORKED OSCILLATORS EXAMPLE

Let \mathbb{G} be a graph and \mathcal{L} its Laplacian matrix. A typical model of a set of networked 2nd-order damped linear oscillators has the form

$$\frac{d}{dt} \begin{bmatrix} \theta(t) \\ \omega(t) \end{bmatrix} = \begin{bmatrix} 0 & I \\ -\mathcal{L} & -\beta I \end{bmatrix} \begin{bmatrix} \theta(t) \\ \omega(t) \end{bmatrix}, \quad (4)$$

where θ and ω are the vectors of phases and frequencies at each node respectively, \mathcal{L} is a graph Laplacian matrix, and β is a damping coefficients (assumed to be the same for all oscillators for simplicity). For example, the swing equations of AC transmission networks has the above form where \mathcal{L} is the imaginary part of the network admittance matrix, and β is each generator’s self damping [12]. In such models, synchrony is the objective, and therefore the “uniform mode” of eigenvalue zero and eigenvector $\mathbb{1}$ (all ones) does not play a role. Thus the dynamical analysis is either done over the subspace $\mathbb{1}^\perp$ of the state space [13], or alternatively \mathcal{L} is replaced by $\mathcal{L} - \alpha \frac{1}{N} \mathbb{1} \mathbb{1}^*$ for a large $\alpha > 0$ to render the uniform mode irrelevant to input-output analysis. We adopt the latter approach so the input-output small-gain theorem 2.1 can be used.

Models like (4) are highly idealized, so it is natural to consider the effect of unmodelled dynamics on properties such as stability. One way of perturbing these models in the manner of Figure 2 is as follows

$$\frac{d}{dt} \begin{bmatrix} \theta \\ \omega \end{bmatrix} = \begin{bmatrix} 0 & I \\ -\mathcal{L} & -\beta I \end{bmatrix} \begin{bmatrix} \theta \\ \omega \end{bmatrix} + \begin{bmatrix} 0 \\ \mathbf{e} \end{bmatrix} u, \quad (5)$$

$$y = \begin{bmatrix} \mathbf{e}^* & 0 \end{bmatrix} \begin{bmatrix} \theta \\ \omega \end{bmatrix}, \quad (6)$$

$$u = \Delta y, \quad \Delta \in \mathbb{H}^\infty, \|\Delta\|_\infty \leq \varepsilon, \quad (7)$$

where \mathbf{e} is a column vector to be described shortly. Note that while (5)-(6) is a state-space model, the perturbation description (7) is written in operator notation since $\Delta \in \mathbb{H}^\infty$ is a dynamical system.

Two possible choices for the vector \mathbf{e} which represent node and edge perturbations respectively are as follows

$$\begin{aligned} \mathbf{e}_k^* &= [0 \dots 0 \quad \overset{k^{\text{th}} \text{ position}}{1} \quad 0 \dots 0], \\ \mathbf{e}_{kl}^* &= [0 \dots 0 \quad \overset{k^{\text{th}} \text{ position}}{1} \quad 0 \dots 0 \quad \overset{l^{\text{th}} \text{ position}}{-1} \quad 0 \dots 0]. \end{aligned} \quad (8)$$

Using \mathbf{e}_k in (5)-(7) represents a perturbation in the *dynamics of node k* , while using \mathbf{e}_{kl} represents a perturbation in the dynamics of *edge (k, l)* . The small-gain theorem 2.1 allows for the study of robust stability of the uncertain system (5)-(7) by replacing $\Delta \in \mathbb{H}^\infty$ with $\Delta \in \mathbb{C}$, and studying the spectrum of the closed-loop “A-matrix”

$$\begin{bmatrix} 0 & I \\ -\mathcal{L} & -\beta I \end{bmatrix} + \begin{bmatrix} 0 \\ \mathbf{e} \end{bmatrix} \Delta \begin{bmatrix} \mathbf{e}^* & 0 \end{bmatrix} = \begin{bmatrix} 0 & I \\ -\mathcal{L} + \mathbf{e} \Delta \mathbf{e}^* & -\beta I \end{bmatrix}, \quad (9)$$

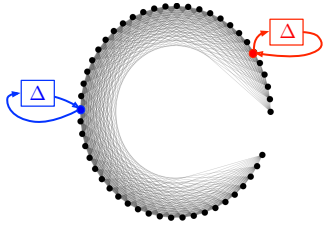
$$\Delta \in \mathbb{C}, |\Delta| \leq \varepsilon.$$

for all possible complex perturbations Δ , i.e. the study of the structured ε -pseudospectrum of the above matrices.

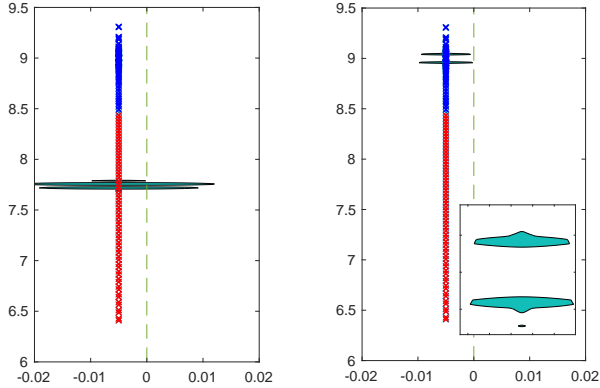
Finally note that although $-\mathcal{L} + \mathbf{e} \Delta \mathbf{e}^*$ is a sub-matrix of the overall A-matrix (9) of the system, their eigenvalues/vectors are closely related by the following general relations

$$A = \begin{bmatrix} 0 & I \\ -\mathcal{L} & -\beta I \end{bmatrix} \Rightarrow \lambda_i(A) = \frac{-\beta \pm \sqrt{\beta^2 - 4\lambda_i(\mathcal{L})}}{2}, w_i = \begin{bmatrix} v_i \\ -\lambda_i(A)v_i \end{bmatrix},$$

where v_i and w_i are the i ’th eigenvectors of \mathcal{L} and A respectively. Note that if the eigenvalues of \mathcal{L} are non-negative (as is the case for Laplacians), then for small



(a) Two different node perturbations in the localized (red) and delocalized (blue) regions.



(b) The structured ε -pseudospectra for perturbations in the localized (left) and delocalized (right) regions together with a subset of the nominal system's eigenvalues (localized and delocalized eigenvalues in red and blue respectively). Here $\varepsilon = 1/2$ in both cases, but the localized perturbation has a much larger effect that can destabilize the system. The inset on the right is a zoomed-in view of the corresponding ε -pseudospectrum.

Fig. 3: The contrast between perturbing the dynamics of nodes in the localized (red) versus the delocalized (blue) regions, together with the resulting structured ε -pseudospectra of the uncertain networked oscillators model (5)-(7). The Laplacian used is of the same structure as that of Figure 1 with 200 nodes and band size 80.

damping β , the eigenvalues of A are all arranged slightly to the left of the imaginary axis with real part $-\beta$ and imaginary parts roughly the square roots of eigenvalues of \mathcal{L} .

Given the above discussion, the robust stability/fragility of the uncertain networked oscillator model (5)-(7) is completely described by the structured ε -pseudospectrum of the matrix (9). The latter is easy to visualize in the complex plane. By way of example, we choose the network of Figure 1 and consider two different perturbations of node dynamics; one for a node in the localized region (shown in red in Figure 3a), and one for the node in the delocalized region (shown in blue in same figure). The structured ε -pseudospectra are shown in Figure 3b for the same value of ε in each case. For a more precise notion of “localized” and “delocalized” regions of the graph, we refer the reader to Definition 4.1 and Assumption 4.2 in the next section.

The results shown in Figure 3 imply that the system's spectrum is much more sensitive to node perturbations in the localized region compared to equally sized perturbations in the delocalized region. For the parameters chosen, the figure also shows that a localized perturbation will destabilize the system. In the networked oscillators example, this will physically imply that these oscillators will lose phase synchrony. Similar observations hold for edge perturbations as shown

in the next section. The analysis will also indicate that this observed contrast in robustness between localized and delocalized perturbations can become arbitrarily large in the large system size limit.

IV. PERTURBATION ANALYSIS

In this section, we give some theoretical insight to indicate that the conclusions from the example of the previous section (for both node and edge perturbations) are likely to be generic for large networks whose Laplacians exhibit localization of some subset of their eigenvectors. The main tool we use is 1st-order spectral perturbation theory, which gives significant insight into why localized eigenvalues are particularly fragile in a large network.

First we begin with a formal definition of localization of eigenvectors. Localization of an eigenvector qualitatively refers to the phenomenon when the mass of an eigenvector is concentrated on a small subset $\mathbb{P} \subsetneq \mathbb{G}$ of a graph \mathbb{G} . Typically, exponential decay of the eigenvector components' magnitudes away from that subset is assumed.

Definition 4.1: Let \mathcal{L} be the Laplacian of a graph \mathbb{G} . $\lambda_i \in \sigma(\mathcal{L})$ is said to be *exponentially localized* (or simply *localized*) if there exists a subset $\mathbb{P}_i \subsetneq \mathbb{G}$ such that the corresponding eigenvector satisfies

$$|v_i(k)| \leq \|v_i\|_2 c q^{\rho(k, \mathbb{P})}, \quad k \in \mathbb{G} - \mathbb{P}, \quad (10)$$

for some constants $c > 0$, $0 < q < 1$, and ρ some distance metric on the graph \mathbb{G} . The set \mathbb{P}_i is called a *peak set* of the *localized* vector v_i .

We empirically observe in all our examples that a graph splits roughly between two subsets of nodes, one which contains all peak sets of all localized eigenvectors, and a complementary set in which there are no peak sets.

Assumption 4.2: A node is said to be *localized* if it belongs to a peak set of some localized eigenvector. We assume the graph to be split between two disjoint subsets $\mathbb{G} = \mathbb{P} \cup \bar{\mathbb{P}}$, where \mathbb{P} contains all peak sets of all localized eigenvectors, and $\bar{\mathbb{P}}$ contains none. \mathbb{P} and $\bar{\mathbb{P}}$ are called the *localized* and the *delocalized* regions of the graph respectively.

The localized and delocalized regions for the example of Figure 1 are denoted by the red and blue bars respectively in Figure 1a.

Definition 4.1 is most meaningful for infinite graphs, and also similar in spirit to *exponential dynamical localization* as defined in [14] in the context of Anderson localization. For finite graphs one can always find constants to satisfy the above bounds for any eigenvector. None the less, the above definition is useful as a guide for the perturbation analysis we develop. Even for large but finite graphs, exponential decay away from peaks is numerically evident for localized eigenvectors such as that shown in Figure 1c. This is how we identified localized versus delocalized eigenvalues/vectors in the examples of the previous section.

A. Spectral Perturbation Analysis

Following the setting of Section III, we want to analyze the behavior of the eigenvalues of the perturbed matrix

$$\mathcal{L} + \mathbf{e}\delta\mathbf{e}^*, \quad (11)$$

where \mathcal{L} is the Laplacian of a network, $\delta \in \mathbb{C}$ is the perturbation parameter, and \mathbf{e} is a vector representing either a single node or edge perturbation as in (8). Note that a scalar $\delta \in \mathbb{C}$ with $|\delta| \leq \varepsilon$ is an exact proxy for a SISO dynamic $\Delta \in \mathbb{H}^\infty$ with $\|\Delta\|_\infty \leq \varepsilon$ according to Theorem 2.1.

Denote the *rank-one* matrix $\mathbf{e}\mathbf{e}^*$ by \mathcal{L}_1 . The perturbed matrix (11) is then

$$\tilde{\mathcal{L}} = \mathcal{L} + \delta \mathbf{e}\mathbf{e}^* = \mathcal{L} + \delta \mathcal{L}_1. \quad (12)$$

Denote the nominal (i.e. those of \mathcal{L}) eigenvalues/vectors by $\{\lambda_i, v_i\}$, and the perturbed eigenvalues/vectors (i.e. those of $\tilde{\mathcal{L}}$ in (12)) by $\{\tilde{\lambda}_i, \tilde{v}_i\}$. For sufficiently small ε and $|\delta| \leq \varepsilon$, the perturbed eigenvalues are analytic functions¹ of δ , e.g. as functions of δ , the perturbed eigenvalues have the form

$$\tilde{\lambda}_i(\delta) = \lambda_i + \lambda_i^{(1)}\delta + \lambda_i^{(2)}\delta^2 + \dots$$

Spectral perturbation theory [15], [16] gives formulas for the coefficients $\lambda_i^{(k)}$ in this expansion. In particular, the first-order coefficient is given by (assuming nominal eigenvectors are normalized: $v_i^*v_i = 1$)

$$\lambda_i^{(1)} = v_i^* \mathcal{L}_1 v_i = v_i^* \mathbf{e}\mathbf{e}^* v_i = (\mathbf{e}^* v_i)^2, \quad (13)$$

where v_i is the nominal eigenvector of the nominal eigenvalue λ_i . We now apply this formula to the cases of node and edge perturbations respectively.

Node perturbations: In the case of perturbations of the dynamics of the k 'th node: $\mathcal{L}_1 = \mathbf{e}_k \mathbf{e}_k^*$, with \mathbf{e}_k given by (8). The formula (13) then simplifies to

$$\lambda_i^{(1)} = v_i^* (\mathbf{e}_k \mathbf{e}_k^*) v_i = v_i^2(k). \quad (14)$$

Note that $v_i(k)$ is the value of the i 'th eigenvector at node k . This leads to 4 possible scenarios depending on whether v_i is a localized/delocalized eigenvector, and whether node k is in its peak set or otherwise.

- Perturbing a localized node k
 - λ_i localized, node- $k \in$ peak set of v_i
 $\Rightarrow v_i(k)$ is large \Rightarrow large changes in λ_i .
 - λ_i localized, node- $k \notin$ peak set of v_i
 $\Rightarrow v_i(k)$ is small \Rightarrow negligible changes in λ_i .
- Perturbing a delocalized node k
 - λ_i delocalized. At any node k , $v_i(k)$ is relatively small
 \Rightarrow small changes in λ_i .
 - λ_i localized, node $k \notin$ peak set of v_i
 $\Rightarrow v_i(k)$ is tiny \Rightarrow negligible changes in λ_i .

Thus the highest sensitivities due to node perturbations are for localized eigenvalues, and in particular those whose peak sets contain that node. Note that the sensitivity (14) can be

¹Technically, this requires \mathcal{L} to have non-repeating eigenvalues. Some modifications are needed in the case of repeated eigenvalues.

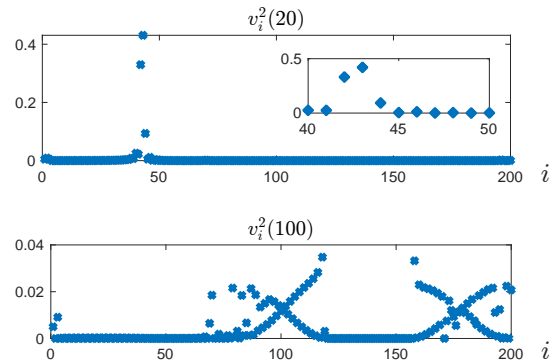


Fig. 4: The sensitivity (14) of the i 'th eigenvalue to node perturbations at a localized node $k=20$ (top figure) and a delocalized node $k=100$ (bottom figure). The worst case sensitivity is about one order of magnitude higher for localized node perturbations compared to those for delocalized nodes. This is consistent with the results shown in Figure 3.

actually “read off” the eigenvector diagram of Figure 1b by choosing the node index, and then examining the value of all eigenvectors at that node. This is shown more clearly in Figure 4 which shows the sensitivity (14) of all eigenvalues to perturbations for specific localized and delocalized nodes respectively. The sensitivity to localized node perturbations is about one order-of-magnitude larger in comparison, and this result is consistent with the observations in the example of Figure 3.

Edge perturbations: A perturbation of the (k,l) 'th edge is represented by the use of $\mathbf{e} = \mathbf{e}_{kl}$ in (8). In this case, formula (13) becomes

$$\lambda_i^{(1)} = v_i^* (\mathbf{e}_{kl} \mathbf{e}_{kl}^*) v_i = (v_i(k) - v_i(l))^2. \quad (15)$$

Delocalized eigenvectors have relatively small magnitudes at any node since the vector is “spread out” over the entire domain. Therefore if λ_i is a delocalized eigenvalue, its sensitivity to any edge perturbations is small. On the other hand, localized eigenvalues have eigenvectors with values of order 1 over nodes in their peak sets, which by Assumption 4.2 occur only in the localized region. Thus the largest edge-perturbation sensitivities (15) occur for (a) edges in the localized region, and (b) for eigenvalues whose eigenvectors have peak sets including the edge’s nodes.

Figure 5 shows an example of edge perturbation sensitivities of all eigenvalues to perturbations of a localized and a delocalized region edge. The edge (20,21) is in the localized region, and we therefore see particularly high sensitivities for only about 4 eigenvalues. Those eigenvalues are localized, and their peak sets include that edge. On the other hand, the edge (100,101) is in the delocalized region, and many more eigenvalues show sensitivities, but of about a factor of 5 lower than the maximum sensitivity of the localized edge perturbation. This is consistent with the trends predicted in the previous paragraph.

This contrast is also evident in the pseudospectra plots shown in Figure 6. The figure shows the ε -pseudospectra for the same two edge perturbation cases. Note that this is the same network of Figure 3. We again see that the

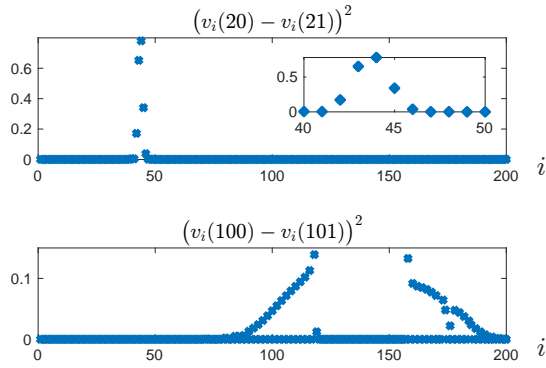
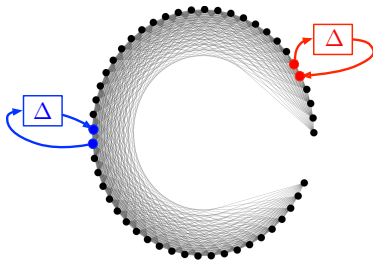
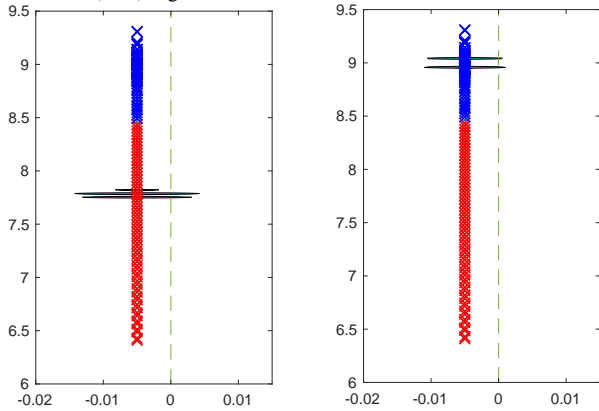


Fig. 5: The sensitivity (15) of the i 'th eigenvalue to edge perturbations in the localized (top figure, edge (20,21)) and the delocalized (bottom figure, edge (100,101)) regions; the latter shows a factor of 5 lower maximum sensitivity in comparison. This is consistent with the corresponding pseudospectral plots shown in Figure 6.



(a) Two different perturbations of edges in the localized (red) and delocalized (blue) regions.



(b) The structured ϵ -pseudospectra for perturbations in the localized (left) and delocalized (right) regions.

Fig. 6: Same setting as Figure 3 but with *edge* rather than node perturbations, and with $\epsilon = 1/6$.

pseudospectrum is more sensitive to perturbations in the localized region versus those in the delocalized region.

The contrast in sensitivities shown in these figures may or may not be significant depending on the specific problem setting. However, it is possible to argue that this contrast can become much larger for larger systems. For large graphs where $N \rightarrow \infty$, the sensitivities (14) and (15) approach zero for nodes/edges in the delocalized region as this region size grows unboundedly, and therefore the magnitude of eigenvectors over any node in the region tends to zero. On the other hand, the sensitivities can remain bounded away from

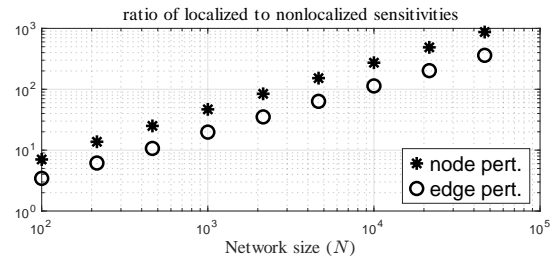


Fig. 7: The ratios of maximum edge and node sensitivities (over all eigenvalues) as computed by the formulas (14) and (15) for the example of Figures 3 and 6. For various network sizes N , the ratio of band size to network size is kept constant (at $1/5$). While localized node and edge sensitivities remain of order 1, delocalized node and edge sensitivities limit to zero (as $N \rightarrow \infty$), thus causing the sensitivities ratios to increase apparently without bound in the limit of large network size.

zero for certain nodes/edges in the localized region. Thus we expect *the contrast between robustness to localized versus delocalized node/edge perturbations to become arbitrarily large in the limit of large network size*. The computations shown in Figure 7 indicate that this is indeed the case for both edge and node perturbations.

V. CONCLUSION

This paper highlights a fragility of certain large networked systems due to localization of Laplacian eigenvectors. The fragility shown in the examples may have significant implications for systems whose dynamics are modeled similarly to (4), such as those of AC transmission networks or oscillator networks more generally. A thorough investigation of such implications is the subject of further research.

In this paper we have not addressed the issue of which graph features cause eigenvector localization. This is also the subject of further research and beyond the scope of the current paper. One conjecture is motivated by features in Figure 1a, where we highlight the indices of the localized nodes in red and delocalized nodes in blue. The latter corresponds to regions of degree homogeneity, while the former are in regions of *degree heterogeneity*, which might play a role as one cause of localization. Clearly, much more work is needed to uncover the causes and implications of this newly-discovered (in networks) fragility phenomenon.

REFERENCES

- [1] Philip W Anderson. Absence of diffusion in certain random lattices. *Physical review*, 109(5):1492, 1958.
- [2] Douglas N Arnold, Guy David, Marcel Filoche, David Jerison, and Svitlana Mayboroda. Localization of eigenfunctions via an effective potential. *Communications in Partial Differential Equations*, 44(11):1186–1216, 2019.
- [3] Simon Félix, Mark Asch, Marcel Filoche, and Bernard Sapoval. Localization and increased damping in irregular acoustic cavities. *Journal of sound and vibration*, 299(4-5):965–976, 2007.
- [4] Alexander Figotin and Abel Klein. Localization of classical waves i: Acoustic waves. *Communications in mathematical physics*, 180(2):439–482, 1996.
- [5] Yann Chalopin, Francesco Piazza, Svitlana Mayboroda, Claude Weisbuch, and Marcel Filoche. Universality of fold-encoded localized vibrations in enzymes. *Scientific reports*, 9(1):12835, 2019.
- [6] Poorva Shukla and Bassam Bamieh. Localization and landscape functions for graph laplacians. in preparation, November 2024.
- [7] F. Bullo. *Lectures on Network Systems*. Kindle Direct Publishing, 1.7 edition, 2024.

- [8] John C Doyle, Bruce A Francis, and Allen R Tannenbaum. *Feedback control theory*. Courier Corporation, 2013.
- [9] Kemin Zhou and John Comstock Doyle. *Essentials of robust control*, volume 104. Prentice hall Upper Saddle River, NJ, 1998.
- [10] Lloyd N Trefethen. *Spectra and pseudospectra: the behavior of nonnormal matrices and operators*. Princeton university press, 2020.
- [11] Diederich Hinrichsen and Anthony J Pritchard. Stability radius for structured perturbations and the algebraic riccati equation. *Systems & Control Letters*, 8(2):105–113, 1986.
- [12] Florian Dörfler and Francesco Bullo. Synchronization in complex networks of phase oscillators: A survey. *Automatica*, 50(6):1539–1564, 2014.
- [13] Emma Tegling, Bassam Bamieh, and Dennice F Gayme. The price of synchrony: Evaluating the resistive losses in synchronizing power networks. *IEEE Transactions on Control of Network Systems*, 2(3):254–266, 2015.
- [14] Michael Aizenman and Simone Warzel. *Random operators*, volume 168. American Mathematical Soc., 2015.
- [15] Bassam Bamieh. A tutorial on matrix perturbation theory (using compact matrix notation). *arXiv preprint arXiv:2002.05001*, 2020.
- [16] Hellmut Baumgärtel. *Analytic perturbation theory for matrices and operators*, volume 64. Walter de Gruyter GmbH & Co KG, 1984.